PNC-TN941 84-06

EXPERIMENTAL STUDY OF HEAT TRANSFER THROUGH COVER GAS IN LMFBR

January, 1984

OARAI ENGINEERING CENTER

POWER REACTOR AND NUCLEAR FUEL DEVELOPMENT CORPORATION

PNC-TN941 84-06

1984 年 1 月

高速炉カバーガス空間の熱伝達に関する実験的研究

布留川　修[*]・古谷　章[**]・服部　達三[***]
井口　達郎[*]

要　　旨

ナトリウム自由液面上部のカバーガス空間における，放射および自然対流の共存した熱伝達に関し実験的研究を行なった。ナトリウム液面からミストの存在するカバーガス空間を通し，上壁に輸送される熱量が測定された。液体ナトリウムおよびミストの付着したステンレス鋼の熱放射率ならびにミスト空間の熱放射特性などの物理量も並行して測定された。これらの物理量測定値をもとに簡易な伝熱量解析法が提案された。伝熱量測定値と解析結果とは，比較的よく一致した。

なお本報告書は，Third International Conference on "Liquid Metal Engineering and Technology in Energy Production" April 1984，Oxford における発表の予稿と同じものである。

* 大洗工学センター高速炉安全工学部高速炉工学室
** 〃 〃 炉心安全工学室
*** 高速増殖炉開発本部

PNC-TN941 84-06

Paper presented at the Third International Conference on "Liquid Metal Engineering and Technology in Energy Production", 1984, Oxford

EXPERIMENTAL STUDY OF HEAT TRANSFER THROUGH COVER GAS IN LMFBR

O. FURUKAWA*, A. FURUTANI*, T. IGUCHI*, N. HATTORI**

* FBR Safety Section, Oarai Engineering Center, PNC

** FBR Development Project, PNC

ABSTRACT

Experimental investigations were performed on the combined radiation and natural convection heat transfer through the cover gas space over the sodium pool. The amount of heat transmitted from the hot sodium to the cold wall through the gas space filled with sodium mist was measured. The thermophysical properties such as the thermal emissivities of liquid sodium and mist-deposited stainless steel and the radiative characteristics of mist-filled space were also measured using especially devised apparatus. The amount of heat transmitted through the space, measured by experiments, was compared with the analytical results based on the measured thermophysical properties. The agreement was comparatively good between the experiment and analysis.

INTRODUCTION

1. The accurate knowledge on the heat transfer to the shield plug through the cover gas is required for the thermal design of LMFBR reactor vessel. During the reactor operation, sodium mist is formed in the cover gas space enclosed with hot sodium pool and surrounding cold walls. The generated sodium mist drifts in the space and attaches to the lower surface of the shield plug and the vessel walls. These mist behavior complicate the heat transfer through the cover gas space.

2. The heat transfer under these conditions is closely related to radiation, natural convection, vaporization, condensation and conduction. The amount of heat transmitted is mainly due to radiation and natural convection.

3. A number of studies were conducted on this subject. Many of them are associated with heat transfer from hot water to cold walls (ref. 1, 2). Only few have been performed for sodium (ref. 3).

4. The present study aims at deriving a simple calculation method to estimate the amount of heat transmitted through the space. Experiments were conducted for the two cases, "mist-free" and "thick-mist". Furthermore, thermophysical properties were measured such as the emissivities of liquid sodium and mist-deposited stainless steel and the radiative characteristics of mist-filled space. These are used to calculate the heat flux by radiation and condensation analytically.

THERMAL EMISSIVITIES

5. The thermal emissivities of pure liquid sodium and stainless steel surfaces facing the mist-filled space were measured by comparing the radiation energy emitted from them with that from a black-body.

6. <u>Liquid sodium</u>. The emissivity of pure liquid sodium ε_{Na} was measured precisely in an inert gas atmosphere. The detailes of the measurement are already reported in ref. 4.

7. The measured total emissivity of liquid sodium ε_{Na} is shown in Fig. 1. The figure shows that ε_{Na} is approximately 0.05 in the temperature range from 180 to 500°C.

8. The measured value of monochromatic emissivity was almost constant in the wavelength range from 2 to 15 μm. The liquid sodium is considered as the gray-body.

9. <u>Mist-deposited stainless steel</u> The mist deposits are chemically changed easily by very small amount of impurities in the cover gas. The emissivity of mist-deposited stainless steel ε_w might changes considerably by the chemical state of the deposits. In the experiment, it is rather hard to keep the specimen surface under the same mist-deposited condition as the stainless steel structures facing the sodium pool in the operating LMFBR.

10. Type-304 stainless steel plates (4.5cm × 4.5cm) were used as the specimen for mist deposition. The specimen was installed in the cover gas space of the test vessel as shown in Fig. 6. After the surface had been covered with mist deposits, the specimen was pulled out to the emissivity measuring port. The environmental gas in the port was freely exchanged with the cover gas in the vessel. Thus, the mist deposits on specimen was maintained under the almost same condition as in the vessel.

11. The mist-deposited surface of the specimen in the port is shown in Fig. 2. The surface of the specimen was almost covered with sodium droplets. The examples of the monochromatic emissivities of the mist-deposited stainless steel are shown in Fig. 3.

12. The emissivity ε_w was estimated to be 0.05

to 0.17. The former value corresponds to pure sodium and the latter to the stainless steel, respectively. However, the deposits were easily contaminated when it was left in the port without deposition of fresh mist. In such a case, the emissivity might become greater than 0.5.

RADIATIVE CHARACTERISTICS OF MIST-FILLED SPACE

13. The radiative characteristics of mist-filled space depend on the mist concentration in the space. The attenuation of radiation energy through the space was measured varing the mist concentration.

14. Mist concentration. A sintered stainless steel filter was set into the cover gas space of the test vessel. A certain volume of the gas was passed through the filter, where the mist was trapped. The mist trap efficiency of the filter had been reported to be greater than 98% (ref. 5).

15. In Fig. 4, the mist concentration C are plotted against the temperature difference ΔT between the sodium surface T_{Na} and the upper wall of the cover gas T_{UW}.

$$\Delta T = T_{Na} - T_{UW}$$

As the design value of T_{Na} in the reactor vessel was 529°C for the Japanese prototype LMFBR "Monju", many experiments were conducted at this temperature. The measured concentrations scattered from 10 to 25 g/m^3 for T_{Na} at 530°C and ΔT exceeding 130°C. We called this case as the "thick-mist". The mean value of 18 g/m^3 was used as the representative one for the thick-mist case.

16. The concentration decreased steeply for ΔT lower than 80°C. It became smaller than the saturated vapor concentration at the sodium pool surface if ΔT was lower than 50°C. It meaned that little mist was formed under this condition. Another test showed that the mist formation could be neglected at T_{Na} lower than 250°C regardless of the ΔT. It was also confirmed by visual observations through a window. These cases were called as the "mist-free".

17. Extinction coefficient of radiation energy. The method to measure the attenuation ratio of the radiation energy is explained in Fig. 5. At first, the test chamber was kept under the mist-free, to measure the radiation energy from the black-body through the chamber I_B, and the background radiation energy I_G. The net incident energy to the detector emitted from the black-body I_o was calculated by

$$I_o = I_B - I_G$$

Likewise, the energy difference I was also measured through the mist-filled chamber.

$$I = (I_B - I_G)_{mist}$$

The value of I gives the energy having passed through the mist-filled space. The attenuation ratio α was given by

$$\alpha = \frac{I_o - I}{I_o} = 1 - \frac{I}{I_o} \qquad \text{..... (1)}$$

The measurements were carried out varying the mist concentration for the same thickness of the mist-filled layer.

18. The extinction coefficient K in a scattering and absorbing layer is defined by

$$I = I_o \exp(-KX)$$

$$K = K_\sigma + K_\alpha \qquad \text{..... (2)}$$

where X is the thickness of the layer and K_σ and K_α are the scattering and absorption coefficients, respectively. Using eq. (1) and (2), α is written as

$$\alpha = 1 - \exp(-KX) = 1 - \exp(-K_c CX) \qquad \text{..... (3)}$$

where K_c is the mass extinction coefficient.

19. The value of K_c was determined by the least squares method using measured value of α for different mist concentrations C. The results are given in Table I, where K_c is 1.8 (m^2/g) at the black-body temperature of 530°C. Then, K is given as 32(1/m) for the thick-mist case.

HEAT TRANSFER THROUGH COVER GAS SPACE

Experimental equipment and procedure

20. The stainless steel vessel (60cm I.D.) shown in Fig. 6 was used for heat transfer experiment. The vessel was connected to a sodium loop and the sodium flow rate to the vessel was 0 to 2 ℓ/min. The cold-trap temperature of the loop had been kept at 150°C.

21. Thermal insulators (30cm thick) and guard heaters were attached to the outer side of the vessel to prevent heat losses from the vessel wall. The temperature of the sodium surface in the vessel T_{Na} was regulated by inserted heaters. The temperature of the upper wall of the cover gas space T_{UW} was controlled by heaters and thermal insulators placed upon the roof of the vessel.

22. The thermocouples located at the two radial positions were moved vertically by the traverse device to measure the temperature distributions in the gas space.

23. The total heat flux through the gas space q_t was measured at the heat flux measuring section, which was also used as the roof of the vessel. The measuring section was composed of a stainless steel plate (4cm thick) and a helium gas layer (0.5cm thick) above it. Twenty-one thermocouples, in total, were attached at the lower and upper surfaces of the plate and the upper wall over the helium gas layer. The total heat flux was calculated

from the temperature difference between the two surfaces of the plate. The experimental conditions are shown in Table 2.

Analytical considerations

24. Mist-free case. The condensation heat transfer may be neglected for mist-free cases because the evaporation rates are small. The total heat flux q_t is expressed by the sum of heat flux of natural convection q_n and radiation q_r.

$$q_t = q_n + q_r \quad \text{..... (4)}$$

25. The sodium pool surface and the upper wall of the cover gas can be considered to form parallel plates with an insulated side wall. The radiation heat flux q_r is calculated by eq. (5) using the measured values of ε_{Na} and ε_w.

$$q_r = \frac{\sigma(T_{Na}^4 - T_{Uw}^4)}{\left(\frac{1}{\varepsilon_{Na}} + \frac{1}{\varepsilon_w} - 1\right) + \frac{1 - F}{1 + F}} \quad \text{..... (5)}$$

where σ is the Stefan-Boltzmann's constant and F is the configuration factor of the parallel plates.

26. The natural convection heat flux q_n is obtained from measured total heat flux q_t, using eq. 4 and q_r calculated by eq. (5).

27. The Nusselt number between upper and lower surfaces of the space N_u and the Rayleigh number R_a are defined by eq. (6). The value of q_n was used to calculate the Nusselt number.

$$N_u = \frac{q_n H}{\lambda \Delta T}, \qquad R_a = \frac{g\beta H^3 \Delta T}{a\nu} \quad \text{..... (6)}$$

where λ is the thermal conductivity, g is the gravitational acceleration, β is the coefficient of thermal expansion, a is the thermal diffusivity, ν the kinematic viscosity, and H the height of the cover gas space. The thermophysical properties are evaluated at the temperature of the core region of the cover gas.

28. Thick-mist Case.

29. Condensation and natural convection heat transfer: Condensation heat flux q_c is expressed by the products of latent heat L and vapor mass flux $\dot{m}_{Na}$, evaporating from the pool surface. Since the Lewis number of sodium vapor is about unity, $\dot{m}_{Na}$ is given by eq. (7).

$$\dot{m}_{Na} = \frac{\rho\, D\, \Delta m}{\ell} Sh = \frac{\lambda}{C_p} \cdot \frac{\Delta m}{\ell} Sh \quad \text{..... (7)}$$

where C_p is the specific heat, ℓ is the characteristic length, Sh is the Sherwood number and Δm is the difference of mass fraction between the sodium surface and the core region of the cover gas. The Nusselt number N_{uo} is defined by eq. (8), for the thermal boundary layer near the sodium surface without mist formation.

$$N_{uo} = \frac{q_n\, \ell}{\lambda(T_{Na} - T_G)} \quad \text{..... (8)}$$

where T_G is the temperature of the core region. As described later, T_G was approximately the mean value of T_{Na} and T_{UW}. Therefore $(T_{Na} - T_G)$ is nearly equal to $\Delta T/2$. From these relations, q_c is given by eq. (9).

$$q_c = L\, \dot{m}_{Na} = q \frac{2L\Delta m}{C_p \Delta T} \frac{Sh}{N_{uo}} \quad \text{..... (9)}$$

30. The core region of the cover gas was filled with sodium mist. It was assumed that the critical super saturation model could be applied for the mist formation. The vapor pressure in the core region was then evaluated to be critical super saturation. The evaporation surface was assumed to be at the saturated vapor pressure. Under these assumptions, the Δm in eq. (9) is expressed as follows

$$\Delta m = m_{sat}(T_{Na}) - S_c m_{sat}(T_G)$$

where $m_{sat}(T)$ is the mass fraction of saturated vapor at temperature T and Sc is the critical supersaturation ratio. The value of Sc was calculated by the theory of Rosner (ref. 6). The ratio (Sh/N_{uo}) for mist formation was assumed 2.0 based on the work of Kumada (ref. 7).

31. As also described later, the behavior of natural convection is changed little by mist formation, q_n derived from eq. (6) can be applied in this case. Substituting q_n into eq. (9), the sum of q_n and q_c is given by

$$q_n + q_c = h\Delta T$$

$$h = \frac{\lambda N_u}{H}\left(1 + \frac{4L\Delta m}{C_p \Delta T}\right) \quad \text{..... (10)}$$

where N_u was calculated by Dropkin's correlation shown in Fig. 8.

32. Radiation heat transfer: The optical thickness of the cover gas space k, is given by

$$k = KH$$

In this experiment, H was 0.14 or 0.27 m and K was approximately 32(1/m), then k became 4.5 or 8.6. The diffusion approximation can be applied for radiation heat transfer under such conditions. The radiation heat flux q_r for infinite parallel plates are given by,

$$q_r = \frac{\sigma(T_{Na}^4 - T_{Uw}^4)}{\frac{3}{4}k + \left(\frac{1}{\varepsilon Na} + \frac{1}{\varepsilon w} - 1\right)} \quad \text{..... (11)}$$

33. Total heat flux: Assuming that each heat

transfer is independent, the total heat flux q_t is given by

$$q_t = q_n + q_c + q_r \qquad \ldots\ldots (12)$$

Dividing eq. (12) by σT_{Na}^4 and letting $\theta = T_{Uw}/T_{Na}$ give the nondimensional total heat flux,

$$\frac{q_t}{\sigma T_{Na}^4} = \frac{1 - \theta^4}{\frac{3}{4}k + \left(\frac{1}{\varepsilon_{Na}} + \frac{1}{\varepsilon_W} - 1\right)} + \frac{4N(1 - \theta)}{k} \qquad \ldots\ldots (13)$$

where N denotes the ratio of convection to radiation.

$$N = \frac{hK}{4\sigma T_{Na}^3}$$

The first term in the right hand side of eq. (13) corresponds to radiation, and the second term the sum of natural convection and condensation heat flux, respectively.

Experimental Results.

34. Temperature distributions. Temperature distribution in the gas space indicates the behavior of natural convection. Vertical temperature distributions are plotted in Fig. 7, for mist-free and thick-mist cases. Similar distributions were formed for both cases, there being a nearly isothermal core region with the thermal boundary layers close to the upper and lower surfaces. The temperature of the core region was approximately the mean value of upper and lower surface temperatures. The distribution is typical of an enclosed fluid layer between horizontal parallel plates heated from below. It was confirmed that the behavior of natural convection was changed little by mist formation.

35. Mist-free Case. The measured values of q_t are plotted according to the relationships derived from the analytical considerations. The results are shown in Fig. 8, with correlation equations. These correlations are generally used for the natural convection heat transfer in an enclosed fluid layer. The experimental results agree well with the correlations.

36. Thick-mist Case. The value of $q_t/\sigma T_{Na}^4$ was calculated for the measured data of q_t. The results are shown in Fig. 9 with the analytical ones. The analytical results is expressed by the band where N and k varies 0.063 to 0.17 and 4.5 to 8.6 respectively, according to the experimental conditions.

37. The analysis showed the same tendency with the experimental results. But it gave a little higher value than the measured one. The difference might be caused by the value of Sc, (Sh/N_{uo}) or K adopted for the analysis. Furthermore, the interaction among the heat transfer mechanisms described before might have influenced the total heat flux. However, the analysis is practical and useful to calculate the amount of heat transmitted under the complicated condition like this, in comparatively good accuracy.

CONCLUSIONS

38. The heat transfer in the cover gas space over the sodium pool surface was studied experimentally.

39. The emissivity of the pure liquid sodium was approximately 0.05. The emissivity of the mist-deposited stainless steel ranged from 0.05 to 0.17 when it was faced directly to the pool surface of sodium and continually exposed to the mist-filled space. But it varied considerably with the chemical change of the deposits when the fresh mist was not deposited continuously.

40. The mist concentration and the extinction coefficient of the radiation energy in the cover gas were measured. The diffusion approximation could be applied to the radiation heat transfer under the thick-mist condition.

41. There was a close simialality between the temperature distributions under mist-free and thick-mist conditions. It was concluded that the behavior of natural convection differed little by mist formation.

42. The measured heat flux agreed well with the sum of the radiation and the natural convection heat flux under the mist-free case. However, the heat transfer mechanism was complicated by mist formation. The simple method was proposed to calculate the total heat flux through the space. The method was based on (1) the critical supersaturation model for mist formation, (2) natural convection heat transfer in the horizontal fluid layer and (3) diffusion approximation for radiation heat transfer. The method predicted the total heat flux in comparatively good agreement with the experimental results.

REFERENCES

1. Clement C.F. and Hawtin P., "Transport of sodium through the cover gas of a sodium cooled fast reactor", Proc. Int. Conf. on Liquid Metal Tech. in Energy Production, Champion, PA, (1976).

2. Ainsworth R.W., Hawtin P., Ralph J.C. and Roberts D.N., "Heat and mass transfer to the cooled roof and walls of a short air-filled cylinder from two concentric pools of water", Proc. Int. Conf. on Liquid Metal Tech. in Energy Production, Richland, WA, (1980).

3. Lemercier G., Elie X. and Morin B., "TRANSFERT DE CHALEUR ENTRE UNE SURFACE LIBRE DE SODIUM LIQUIDE ET UN TOIT METALLIQUE SEPARES PAR UN GAZ INERTE", DRP/SEMTR/Cad., R. 604, (1970).

4. Hattori. N., Trans. JSME. (Ser. B), vol 49, No. 447, (1983), pp. 2493 ~ 2496, (in Japanese).

5. Himeno Y. and Takahashi J., J. Nucl. Sci. and Tech., vol 17, (1980), pp. 404 ~ 412.

6. Rosner D.E., "Enhancement of diffusion-limited vaporization rates by condensation within the thermal boundary layer", Int. J. Heat and Mass Transfer, vol 10, (1967), pp. 1267 ~ 1279.

7. Kumada T. and Ishiguro R., "Sodium evaporation into a forced argon flow, (II)", J. Nucl. Sci. and Tech., vol 15, (1978), pp. 912 ~ 918.

Table 1. Extinction Coefficient of Mist-filled Space

Temperature of Black body (°C)	Wavelength (μm)	K_c (m^2/g)
300	2.5 ~ 8.5	1.92
	5.0 ~ 8.5	1.87
	7.5 ~ 15	1.55
	average	1.78
530	2.5 ~ 8.5	2.22
	5.0 ~ 8.5	1.99
	7.5 ~ 15	1.36
	average	1.83
800	2.5 ~ 8.5	1.80
	5.0 ~ 8.5	1.50
	7.5 ~ 15	1.35
	average	1.48

Table 2. Experimental Conditions

	Mist-free case	Thickmist case
Temp. of sodium surface T_{Na}(°C)	250	530 ~ 580
Temp. of upper wall of cover gas space T_{Uw}(°C)	100 ~ 140	240 ~ 480
Cover gas	Argon or Herium	Argon
Height of cover gas space H(cm)	14 ~ 27	
Pressure of cover gas P (Pa)	11×10^4 ~ 14×10^4	
Sodium flow rate (cm^3/S)	0 ~ 30	
Temp. of Cold Trap(°C)	150	

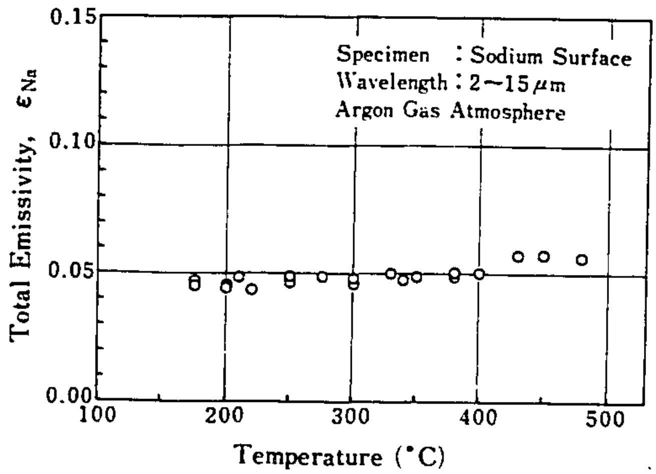

Fig. 1 Total Emissivity of Liquid Sodium

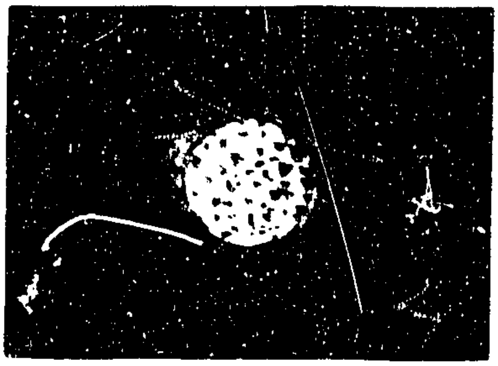

Fig. 2 Mist-deposited Stainless Steel

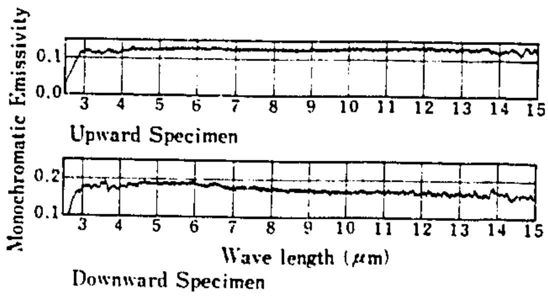

Fig. 3 Monochromatic Emissivity of Mist-deposited Stainless Steel

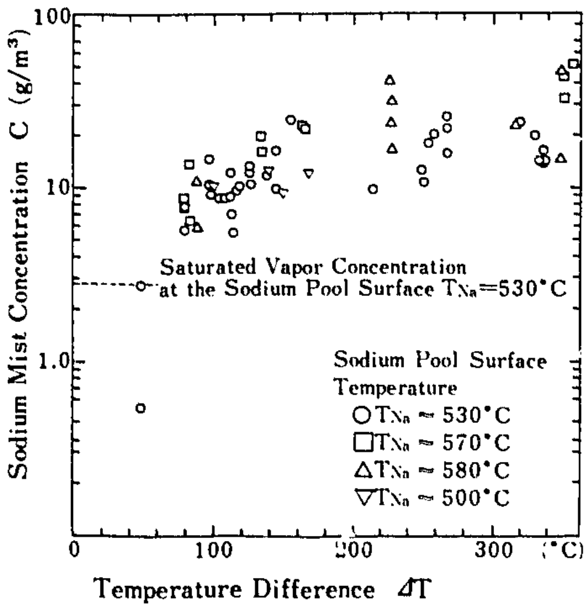

Fig. 4 Mist Concentration

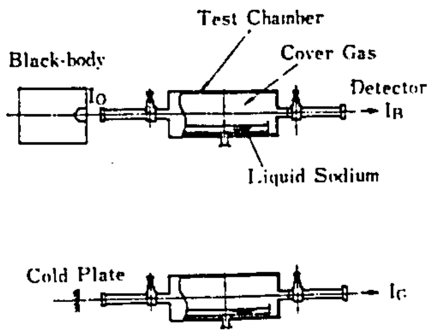

Fig. 5 Method to Measure the Attenuation Ratio

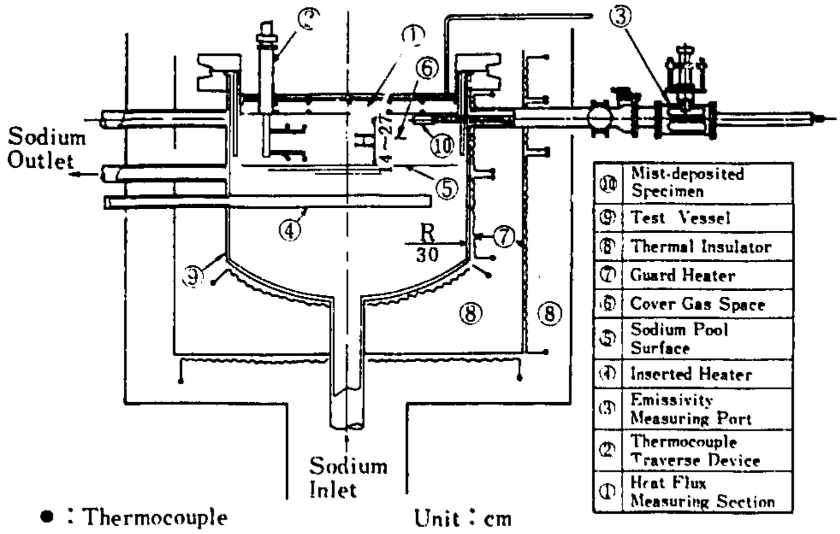

Fig. 6 Test Vessel

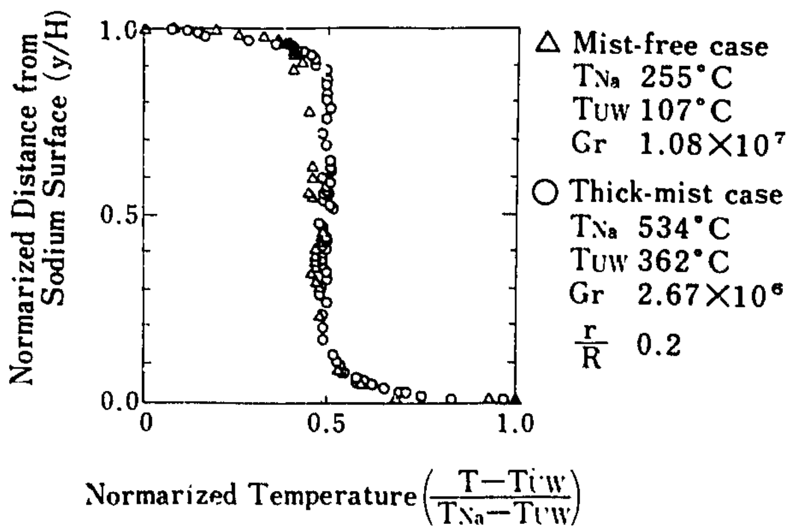

Fig. 7 Typical Temperature Distribution in the Cover Gas Space

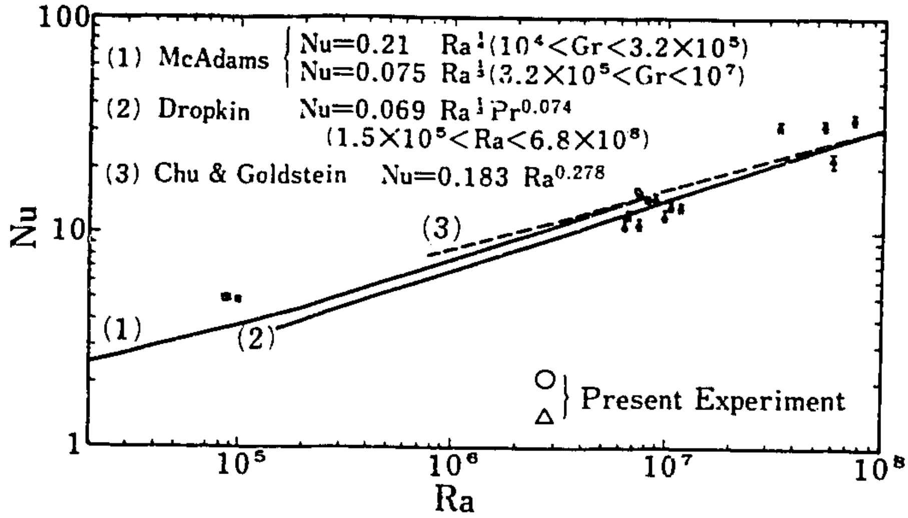

Fig. 8 Experimental Data and Correlation Equations for Mist-free Case

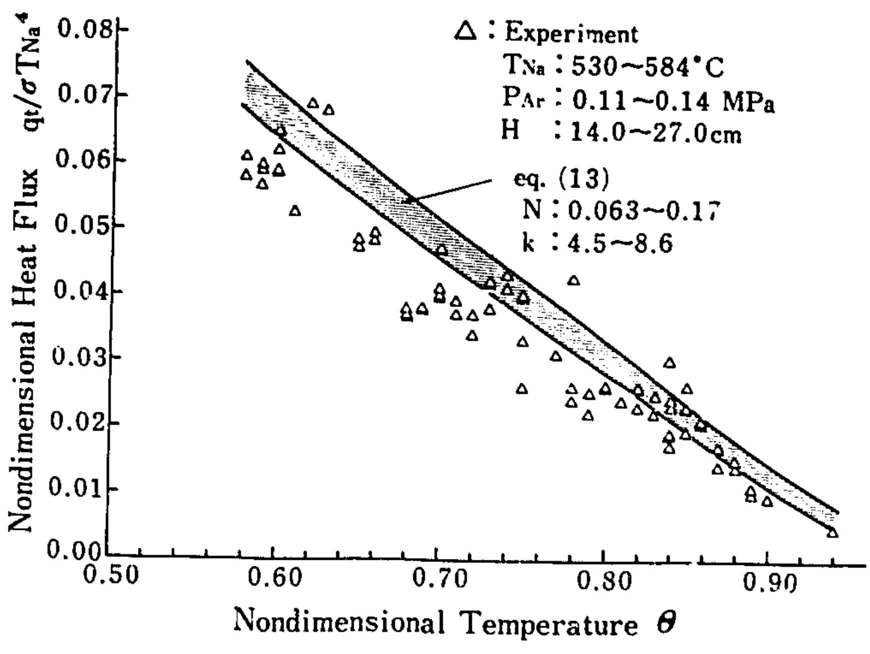

Fig. 9 Nondimensional Heat Flux for Thick-mist Case